

## A New Method to Estimate Thermal Conductivity of Polymer Composite Using Characteristics of Fillers

Hui Joon Park, Tae Ann Kim, Raehyun Kim, Junkyung Kim, Min Park

Photo-electronic Hybrids Research Center, Korea Institute of Science and Technology, Hwarangno 14-gil 5, Seoungbuk-gu, Seoul 136-791, Korea

Hui Joon Park and Tae Ann Kim contributed equally to the work.

Correspondence to: M. Park (E-mail: minpark@kist.re.kr)

**ABSTRACT:** In this work, a new method to estimate the thermal conductivity of polymer composite was suggested. For this purpose, polymer composites composed of high-density polyethylene (HDPE) and boron nitride (BN) were prepared by twin-screw extruder melt-mixing, followed by compression molding technique, and their microstructure was investigated by material simulation. Consequently, the  $C_f$  parameter of Agari and Uno equation, which represents an ease in forming conductive chains, was quantified by “Structure factor (related with conductive pathway)” and “Interfacial factors (related with thermal resistance)”, ultimately helping us evaluate the thermal conductivity of arbitrary composite system. © 2012 Wiley Periodicals, Inc. *J. Appl. Polym. Sci.* 129: 965–972, 2013

**KEYWORDS:** composites; theory and modeling; thermal properties

Received 19 March 2012; accepted 21 September 2012; published online 22 November 2012

**DOI:** 10.1002/app.38653

### INTRODUCTION

As the importance of thermal management in modern electronic technologies has been increased, the need to the new types of engineered materials that can satisfy the various requirements for the thermal properties have been increased.<sup>1–5</sup> Among various candidates, polymer hybrids, composed of inorganic filler having desired thermal properties, and polymer matrix having easy processability, have attracted out attentions due to their versatility that cannot be achieved by single-component materials.<sup>6–13</sup>

Generally, to design the multi-component materials having the intended properties, the proper amount of experimental screening tests<sup>14,15</sup> should be harmonized with the theoretical anticipation,<sup>16–20</sup> because the excessive experimental tests always come with the waste of resources and the calculation-biased works often induce the significant deviation from the targeted properties. Therefore, developing practical models that can help us to precisely estimate the thermal properties of hybrids is one of the most important tasks in this field, and this can be realized by incorporating physical ideas, obtained from both experiments and calculation, into semi-empirical models.

For this purpose, in this work, we have studied an effective method, which can be utilized to predict the thermal conductivity of multi-component materials such as polymer hybrids. Based on the parameters determined from both experimental

and simulation results, we could suggest a way to estimate the thermal conductivity of polymer hybrids according to the characteristics of fillers. The Hybrid system, composed of boron nitride (BN) filler and high-density polyethylene (HDPE) matrix, was chosen as the experimental system, and the material simulation was performed to describe the microstructure of the BNs in a PE matrix. Finally, Agari and Uno equation and its parameters<sup>21,22</sup> were utilized as tools to combine both methods, ultimately providing a practical model for the estimation of thermal conductivity.

It has been known that the polymer composite having high thermal conductivity can be obtained by maximizing the formation of conductive networks while minimizing the heat resistance along the heat pathways. Therefore, in the first section of this work, we have focused on the effect of the shape of filler on thermal conductivity to maximize heat flow pathways. In the following section, the effect of thermal resistance at the interface between filler and matrix was studied by modifying the surface of BN fillers to find out the relation between the heat resistance and thermal conductivity in their heat pathways.

### EXPERIMENTAL

#### Materials

Polymer matrix utilized in this study was a HDPE from Korea Petrochemical Company. Three kinds of BNs (PT110, PT120,

Additional Supporting Information may be found in the online version of this article.

© 2012 Wiley Periodicals, Inc.

and NX1) from GE Advanced Ceramics were used as fillers, and hereafter they are denoted as BN1, BN2, and BN3, respectively. The shapes of those BN fillers are shown in SEM images (Hitachi, S-4200, 10 kV) in Supporting Information Figure S1 and their sizes are 45, 12, and 0.5  $\mu\text{m}$ , respectively. The detailed dimensions are summarized in Supporting Information Table S1. PT grades (BN1 and BN2) have the same chemical composition, and NX grade (BN3) has  $\sim 1\%$  higher oxygen content than PT grade.

### BN Surface Modification

BN powders were first calcinated in the high temperature furnace. The temperature of furnace was increased from 25°C to 850°C for 2 h, then stayed at 850°C for 8 h and finally ramped down to 25°C over 2.5 h. Silane coupling agent (*n*-propyltriethoxysilane, 0.5 g) was added to mixture of distilled water (33 ml) and ammonium hydroxide ( $\text{NH}_4\text{OH}$ , 17 ml), and then 5 g of calcinated BN powders were treated by this solution at 80°C for 12 h. After treated, it was centrifuged at 50,000g for 15 min and washed by the mixture of distilled water and ammonium hydroxide. This washing step was repeated at least two times to remove untreated silane compound. Those silane compound-treated fillers were dried in vacuum to remove residual solvent at 70°C for 1 day and stored at 70°C to protect filler surface from moisture. The changes of heat capacity of fillers after surface treatment were measured by Differential Scanning Calorimeter (DSC, Perkin Elmer), and the characteristics of the surface of the filter were inspected by Fourier Transform Infrared Spectroscopy (FTIR, Perkin Elmer) with attenuated total reflectance (ATR). The amount of molecules attached to BN fillers after surface treatment was estimated by Thermogravimetric Analysis (TGA, TA Instrument, TA 50). The samples mounted on the pan were heated from 30°C to 800°C at the heating rate of 10°C  $\text{min}^{-1}$ .

### Composite Sample Preparation

Both fillers and polymers were dried in vacuum before mixing at 80°C for 12 h. After dried, the polymer powders were mixed with BN fillers using Henschel-type mixer (Hung-bo Tech, Korea) for 15 min (4000 rpm) at desired volume fraction. Those compounds were further mixed by twin-screw extruder (BAUTEK, L/D = 40, D = 19 mm) at 200°C and 200 rpm to provide homogeneous quality. The resultant mixtures were in the form of pellet and they were molded into specimens having the dimension of 80 mm length, 40 mm width and 2 mm thickness by compression molding technique (Tetrahedron, MTP-8) at 180°C and 400 psi for 40 min. The microstructures of BN fillers in composite sample were investigated by materials simulation package, MacroPac (Oxmat, UK), and the detailed information will be explained in results and discussion section.

### Thermal Conductivity Measurement

The thermal conductivity was measured by TC-30 (Mathis Instruments Ltd.) based on the modified hot wire method (ASTM C1113).<sup>23,24</sup> For the accurate measurement, the samples have to be larger than the heating strip (60 mm  $\times$  10 mm) and their thickness have to be thicker than 2 mm. Using this tool, thermal effusivity, and conductivity could be measured at the same time. The proper measurement time was chosen by blotter

method<sup>25</sup> and we could estimate thermal conductivity of samples without knowing their density and heat capacity using this method.

The calibration curves were drawn by matching the effusivity of standard samples with their thermal conductivity. Based on these calibration curves, the thermal conductivity of arbitrary samples could be calculated. All the measurements were repeated at least three times and over four different samples were prepared to evaluate each specific condition. All those measurements were performed at  $30 \pm 1^\circ\text{C}$ .

## RESULTS AND DISCUSSION

### Dimensional Factor of Filler to Estimate the Thermal Conductivity

In order to develop a practical method to estimate the thermal conductivity of polymer composite, we should be able to answer the question, "how efficiently the heat flow pathways can be formed in the composite system?" For this purpose, we first investigated the effects of geometry of the fillers on the formation of conductive pathways. Three different types of BN having high thermal conductivity were selected as fillers, and HDPE was utilized as polymer matrix. Our analysis was based on the model proposed by Agari and Uno about thermal conduction in composite materials.<sup>21,22</sup>

$$\log(\lambda) = V \cdot C_f \log\left(\frac{\lambda_2}{C_p \lambda_1}\right) + \log(C_p \lambda_1) \quad (1)$$

where  $\lambda$ ,  $\lambda_1$  and  $\lambda_2$  are the thermal conductivity of composite, matrix and filler, respectively.  $C_p$  represents a measure of the effect of the particles on the secondary structure of the polymer, such as crystallinity and the crystal size of the polymer matrix.  $C_f$  reflects the ease in forming conductive pathways.  $V$  is the volume fraction of filler.

Figure 1 shows the thermal conductivity of composites according to volume fraction of fillers. The solid lines are linear fit of experimental results to eq. (1), and both  $C_p$  and  $C_f$  were calculated by the intercept and slope of those linear curves, respectively. Because all the composite samples were fabricated by the same HDPE matrix, all the  $C_p$  values are almost identical. Particularly, our attention was focused on the variation of  $C_f$  values, which are closely related with the formation of conductive pathways in the hybrid system. All the BN fillers used in this work are primarily composed of single-crystal hexagonal plates and all the composite samples were prepared by the same processing conditions, therefore the thermal resistances at the interface between BN and HDPE are almost similar in all samples. Even though BN3 has slightly higher oxygen contents, about 1% difference is expected to give negligible effect on the surface of filler. Our results show that the composite systems composed of BN1 having the largest dimension give the highest  $C_f$  values, which represents that the largest BN1 filler is the most efficient in maximizing the formation of conductive networks. Based on these preliminary results, we speculated that the  $C_f$  could be quantified by the dimension of fillers and consequently used as a guideline to estimate thermal conductivity of polymer composite. For this purpose, we investigated the microstructures of

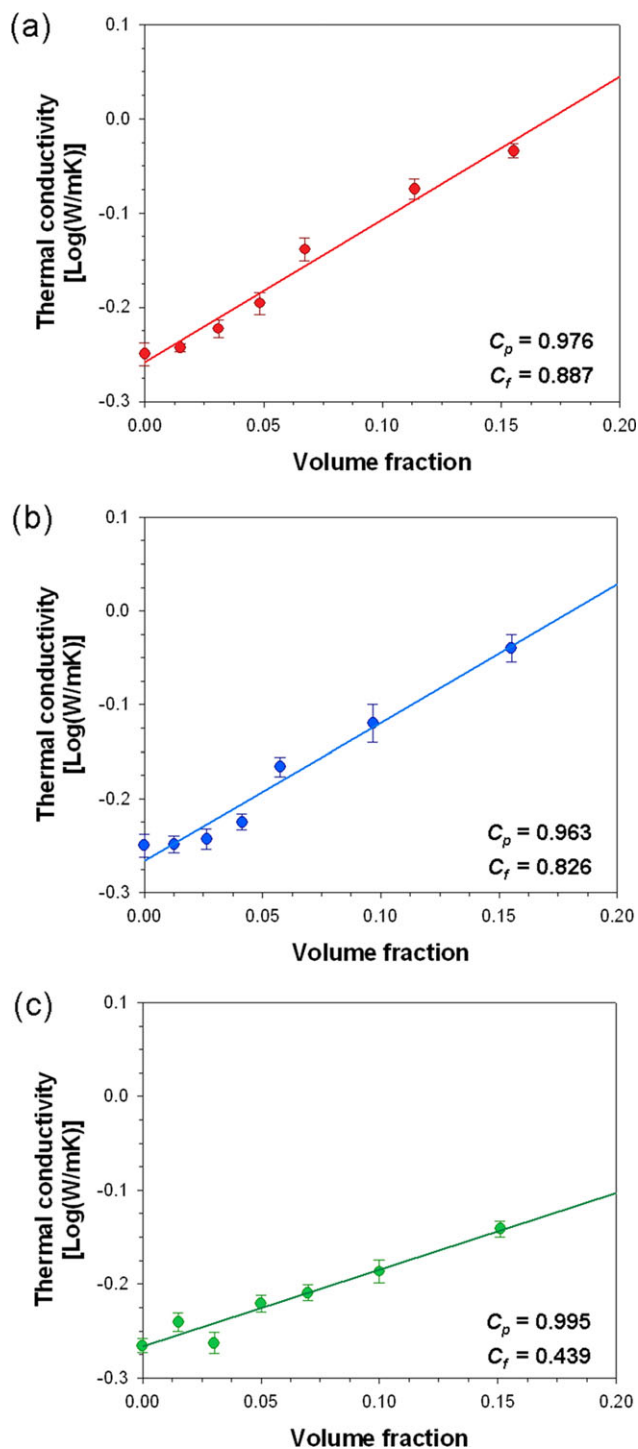


**Figure 1.** Thermal conductivity (log scale) as a function of volume fraction; (a) BN1 (45  $\mu\text{m}$ )-HDPE composite, (b) BN2 (12  $\mu\text{m}$ )-HDPE composite and (c) BN3 (0.5  $\mu\text{m}$ )-HDPE composite. Filled circle represents the measured thermal conductivities of BN1, BN2 and BN3 systems, and the solid line represents a theoretical fit based on Agari and Uno equation.  $C_p$  and  $C_f$  values for each composite system are inserted in each graph. [Color figure can be viewed in the online issue, which is available at [wileyonlinelibrary.com](http://wileyonlinelibrary.com).]

fillers in the composite according to their dimensions by simulating their packing behavior in the matrix.

The simulation was performed by MacroPac (Oxmat, UK) program.<sup>7,26</sup> In this simulation, BN fillers are described by square-shaped plates, of which dimension has lognormal distribution, and those fillers are randomly generated and packed in the simulation box until simulation algorithm meets the stopping condition. Because the main purpose of simulation is to mimic the thermal conduction pathway formation in the matrix, we defined a parameter, average contact number, which means the average number of adjacent filler that an arbitrary filler contacts. Finally, the relation between this value and the experimentally obtained  $C_f$  were demonstrated.

In order to calculate the average contact number of fillers in the matrix, the cut-off distance, which determines whether fillers are connected, should be set first. In our simulation, the cut-off distance was calculated by equating the heat capacity of the plate with that of surrounding matrix, ultimately being comparable to the thermal diffusion length in the following equation.<sup>27</sup>

$$V_1 \cdot C_1 = V_2(r) \cdot C_2 \quad (2)$$

where  $V_1$  is the volume of a filler,  $V_2(r)$  is the volume of the surrounding matrix within thermal diffusion length  $r$ ,  $C_1$  is the heat capacity of the BN filler (1.835  $\text{J cm}^{-3} \text{K}^{-1}$ , provided by manufacturer), and  $C_2$  is the heat capacity of the HDPE matrix (1.384  $\text{J cm}^{-3} \text{K}^{-1}$ ). The heat capacity of HDPE matrix  $C_2$  was calculated by measuring the effusivity and thermal conductivity of pristine polyethylene sample using the following equation; effusivity ( $\text{W s}^{1/2} \text{m}^{-2} \text{K}^{-1}$ ) = [thermal conductivity ( $\text{W m}^{-1} \text{K}^{-1}$ )  $\times$  heat capacity ( $\text{J cm}^{-3} \text{K}^{-1}$ )]<sup>1/2</sup>. The volume of the surrounding matrix is represented in Supporting Information Figure S2 and the calculated thermal diffusion length, i.e., the cut-off distance, of BN2 system is 0.334  $\mu\text{m}$ , as an example.

The comparison between real sample and simulation space is summarized in Supporting Information Figure S3. To represent the length (80 mm) and width (40 mm) of real composite samples, the periodic boundaries were applied to our simulation space in both  $x$  and  $y$  directions. Therefore, these dimensions cannot give any noticeable effects on our simulation results. Different with those infinite soft boundaries, the planes perpendicular to the  $z$ -axis were set to be hard boundaries to mimic the processing condition such as compression molding. Because those hard boundaries inevitably give much smaller space compared with the thickness of real sample (2 mm), we checked the effect of the size of simulation box in  $z$  direction on the average contact number that we are targeting to calculate here. As shown in Supporting Information Figure S4, the average contact numbers of BN2 system were almost constant over 30  $\mu\text{m}$  thickness; therefore the size of simulation box in  $z$  direction was fixed to 30  $\mu\text{m}$ . Following the same procedures, the thickness of simulation boxes of BN1 and BN3 systems are 100 and 3  $\mu\text{m}$ , respectively.

Another important factor to realistically simulate the polymer composite system is the degree of orientation of fillers in

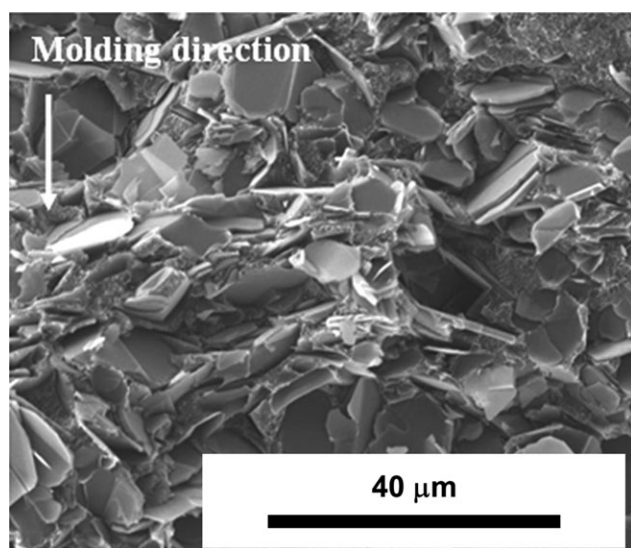


**Figure 2.** SEM image of the cross section of the BN2 composite at 13.5% volume fraction of filler.

matrix.<sup>28–30</sup> Figure 2 shows that BN fillers are perpendicularly oriented to the direction of uniaxial compression molding due to the applied pressure and their plate-shape geometry. Hence, the fillers generated in simulation box should be packed with the orientation perpendicular to  $z$ -axis as much as possible. To make the fillers be oriented to that direction, we shook the simulation box in  $z$  direction and gradually increased the thickness of simulation box to the desired value (e.g., 30  $\mu\text{m}$  in BN2 system). Using this method, we could simulate highly oriented filler system. Supporting Information Figure S5 shows the degree of orientation of fillers according to the step size, which represents the increased thickness of the simulation box during each shaking step. The step size, applied to our simulation, is 2.5, providing highly oriented fillers in the simulation box.

The resultant simulation parameters utilized to demonstrate the microstructure of fillers are summarized in Supporting Information Figure S6. In our calculation, we need to fix the volume fraction of filler only to consider the dimensional effect of fillers such as size and shape by excluding their density effect. As an example, the calculated average contact numbers of BN1, BN2, and BN3 systems at 13.5% volume fraction are 2.36, 2.97, and 15.51, and these values are paired with the aforementioned experimental  $C_f$  values shown in Figure 1 and Table I (0.887, 0.826, and 0.439, respectively). The trends of average contact number at different volume fraction were described in Supporting Information Figure S7 for reference. In the composite systems having the smaller contact number, the phonons have little chance to meet the thermal barriers between heterogeneous phases, which induce their scattering, thus they have higher  $C_f$  values, which represent the better conductive pathway formation. Consequently, we could successfully quantify the  $C_f$  value of eq. (1) with the dimensional factor of filler, i.e., average contact number (Supporting Information Figure S7), which will ultimately guides us to estimate the thermal conductivity of the composite. Meanwhile, there are several prerequisites for this approach. Firstly, fillers should have the similar interfacial con-

**Table I.** The Summary of  $C_f$  and Average Contact Number of BN Systems

	$C_f$	Average contact number <sup>a</sup>
BN1 composite (Filler dimension: 45 $\mu\text{m}$ size, 1 $\mu\text{m}$ thickness)	0.887	2.36
BN2 composite (Filler dimension: 12 $\mu\text{m}$ size, 0.6 $\mu\text{m}$ thickness)	0.826	2.97
BN3 composite (Filler dimension: 0.5 $\mu\text{m}$ size, 0.03 $\mu\text{m}$ thickness)	0.439	15.51

<sup>a</sup>The inverse values of average contact numbers are structure factors in this work. Average contact numbers in this table are calculated from the composites having 13.5% volume fraction. Average contact numbers are changed according to the volume fraction of filler.

dition. The systems having different interfacial thermal resistance will be discussed in the next section. Secondly, the average contact number should be calculated from the composite systems having the same composition to exclude the density effect of filler on thermal conductivity, as discussed. Thirdly, the cut-off distance should be set to be the thermal diffusion length of the filler that has the smallest surface area to assume that the propagation speed of phonon in all the system is the same.

To further validate our simulation results, the diffusivity of composite was analyzed by both simulation and experimental methods. Simulation was performed by the diffusion module in MacroPac. In the diffusion module, each edge of the simulation box is divided into 100 equal segments providing  $10^6$  3D units, and those units become filled or empty depending on the existence of the filler in that space. The filled units are considered as conductors, and the empty ones are considered as insulator. Next, the program randomly generates the particles which can be considered as phonons and track their propagations through the filled units considered as conductors. Using this module, we could calculate the squared moving distances of particles

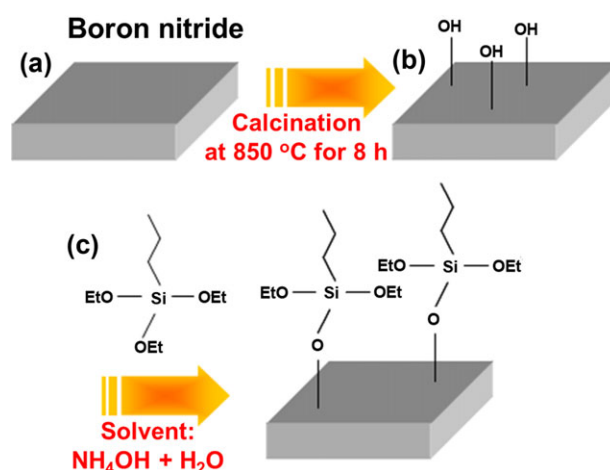


**Figure 3.** The schematic procedures about the surface modification of boron nitride (STBN). [Color figure can be viewed in the online issue, which is available at [wileyonlinelibrary.com](http://wileyonlinelibrary.com).]

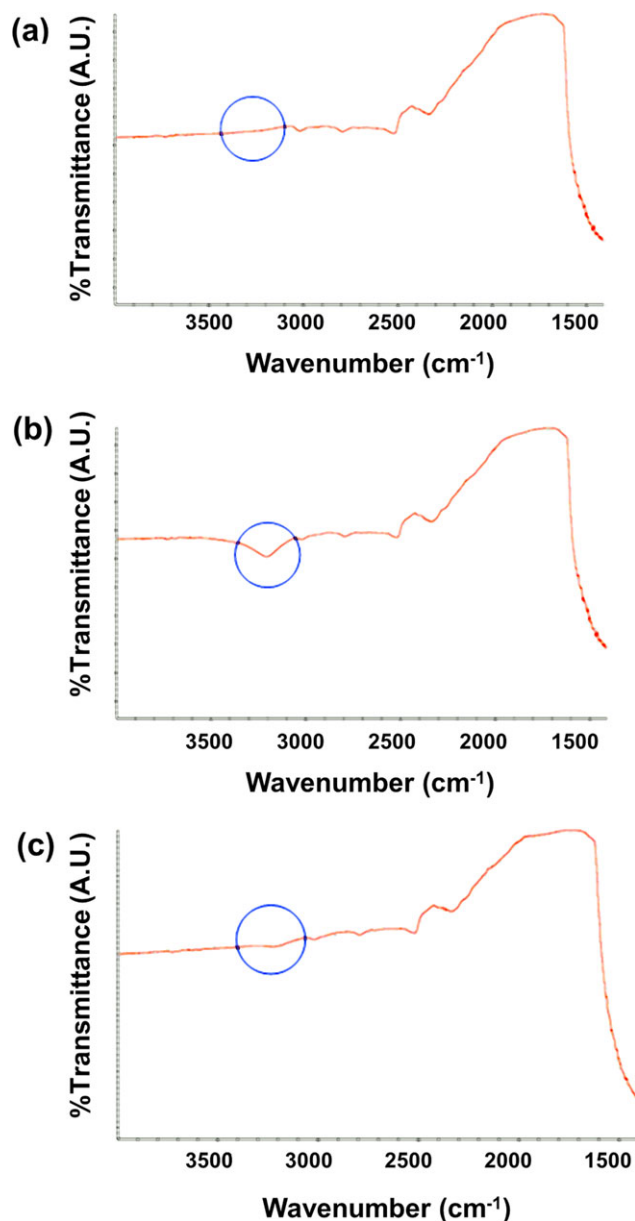


**Figure 4.** IR spectra of BN fillers: (a) BN1, (b) calcinated BN 1, and (c) BN 1 modified by silane compound. BN1 case is shown as a representative. [Color figure can be viewed in the online issue, which is available at [wileyonlinelibrary.com](http://wileyonlinelibrary.com).]

according to steps, which correspond to time, and these values represent the diffusivity of composite. The composite systems in the diffusion module are shown in Supporting Information Figure S8. Since the thermal conductivity measured by the tool (TC-30) is uniaxial property in through-plane direction, the diffusivity calculated in *z*-direction was only chosen for comparison. The calculated diffusivities of BN1 and BN2 systems having 13.5% volume fraction of filler are  $3.80 (\pm 0.08) \times 10^{-9}$  and  $3.32 (\pm 0.07) \times 10^{-9} \text{ m}^2 \text{ s}^{-1}$ , respectively. BN3 system was excluded due to its different oxygen content. Meanwhile, the experimental diffusivity can be obtained by measuring effusivity and thermal conductivity of the samples;

$$\text{Diffusivity}(\text{m}^2/\text{s}) = \frac{[\text{Thermal conductivity} (\text{W}/\text{mK})]^2}{[\text{Effusivity} (\text{Ws}^{1/2}/\text{m}^2\text{K})]^2} \quad (3)$$

Experimental diffusivities of BN1 and BN2 systems having the same volume fraction of fillers showed the same trend with simulation results and their values were  $6.75 (\pm 0.14) \times 10^{-7}$  and  $6.27 (\pm 0.21) \times 10^{-7} \text{ m}^2 \text{ s}^{-1}$ , respectively. From these results, we could confirm that the propagation of phonon is much faster in the composite system having smaller average contact number, which comes with higher  $C_f$  value. In our simulation, because the speed of phonon was not specified and the polymer matrix was considered as perfect insulator, their absolute values cannot be matched each other.

#### Interfacial Factor to Estimate the Thermal Conductivity

Until now, we have shown that  $C_f$  parameter of eq. (1), which will be used as a guideline to estimate the thermal conductivity of composite system, can be evaluated by the dimensional factor of fillers. In our former analysis, we supposed the same interfacial conditions between filler and matrix in all composite systems as a prerequisite to separate out those dimensional

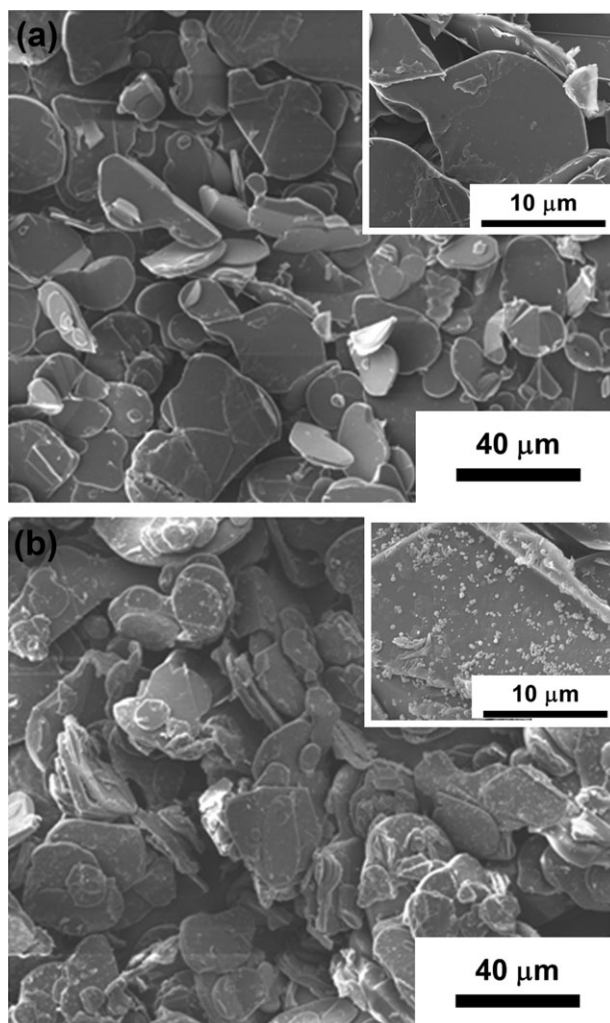


**Figure 5.** SEM images of (a) pristine BN and (b) surface modified boron nitride (STBN). BN1 case is shown as a representative.

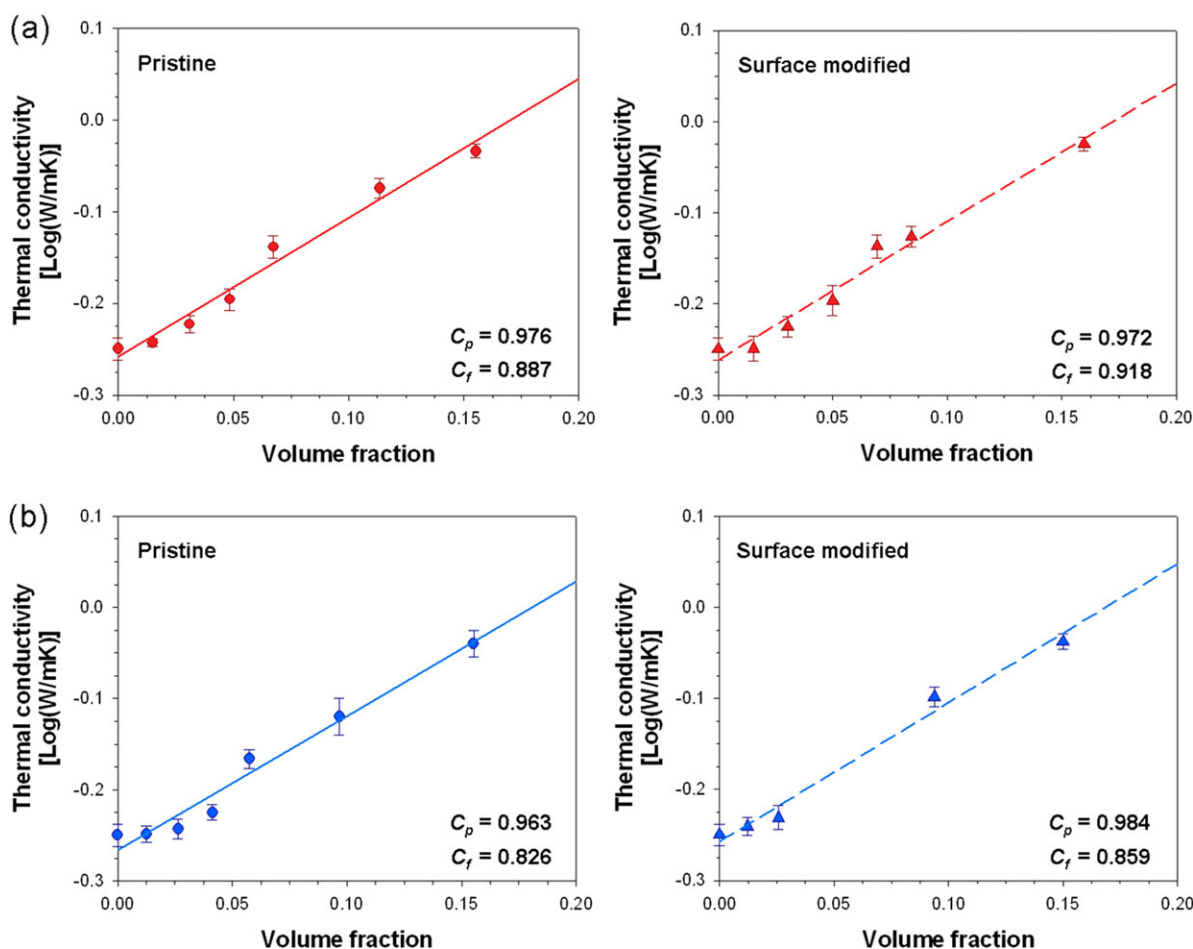


**Figure 6.** The thermal conductivity (log scale) as a function of volume fraction; (a) BN1–HDPE composite (pristine) and STBN1–HDPE (surface modified), (b) BN2–HDPE composite (pristine) and STBN2–HDPE composite (surface modified). Filled circle and triangle represent the measured thermal conductivity, and the solid and dashed lines represent a theoretical fit based on Agari and Uno equation.  $C_p$  and  $C_f$  values for each composite system are inserted in each graph. [Color figure can be viewed in the online issue, which is available at [wileyonlinelibrary.com](http://wileyonlinelibrary.com).]

parameters. In contrast, in this section, we investigated the effect of those interfacial factors on  $C_f$  parameter to complete the comprehensive understanding about the  $C_f$  parameter. For this purpose, the surfaces of BN1 and BN2 fillers were modified by silane compound,<sup>31</sup> and their effects on thermal properties of composite system were studied. This surface treatment improves the hydrophobicity of fillers, ultimately increasing their affinity to HDPE matrix and decreasing potential voids at the interface between filler and matrix. The overall schemes about the surface treatment are depicted in Figure 3. IR spectra of the calcinated BN in Figure 4b shows a broad peak near 3250  $\text{cm}^{-1}$  which does not appear in Figure 4a, indicating that -OH groups are attached to the surface of BN. This broad peak disappears after treating the calcinated BN with silane compound (Figure 4c). The modified surface of BN is further evaluated by Thermogravimetric Analysis (Supporting Information Figure S9) and SEM images (Figure 5).

The thermal conductivities of composite samples composed of those surface-treated BN fillers (hereafter denoted as STBN) are plotted as a function of the volume fraction ( $V$ ) to calculate  $C_f$  values (Figure 6). Our results show that those  $C_f$  parameters are

slightly increased after modifying the filler–matrix interface, which represents that the formation of conductive pathways through fillers becomes easier in the modified system.<sup>32</sup>

Because it is not easy to directly calculate the thermal resistance at the filler–matrix interface due to the experimental difficulties, we alternatively investigated the critical thermal resistance to estimate the variation of thermal resistance at the filler–matrix interface. We have already shown that composite systems satisfy the eq. (2) in thermal equilibrium. The thermal diffusion length  $r$  in eq. (2) can be expressed in terms of diffusivity of phonon through interface,  $D$ , and the characteristic time for cooling of a filler,  $t$ ;  $r = (D \cdot t)^{1/2}$ . Additionally, the cooling time of the filler is given by the ratio of the heat capacity of filler to the total thermal conductance of the filler–matrix interface;<sup>27</sup>

$$\tau = \frac{V_1 \cdot C_1}{S_1 \cdot G} \quad (4)$$

where  $S_1$  is the surface area of a filler and  $G$  is the thermal conductance per unit area of the filler–matrix interface. The thermal conductance,  $G$ , is the reciprocal of the thermal resistance

**Table II.** The Summary of  $C_f$  and  $G_c$  Values of BN and STBN Systems

		BN1 system (45 $\mu\text{m}$ size, 1 $\mu\text{m}$ thickness)	BN2 system (12 $\mu\text{m}$ size, 0.6 $\mu\text{m}$ thickness)
$C_f$	BN	0.887	0.826
	STBN	0.918	0.859
Ratio (STBN/BN)		1.035	1.040
$G_c(\text{MW m}^{-2} \text{K}^{-1})$	BN	9.259	1.698
	STBN	9.423	1.735
Ratio (STBN/BN) <sup>a</sup>		1.019	1.022

<sup>a</sup>Interfacial factors in this work.

that we want to know. Therefore, eq. (2) can be converted to eq. (5).

$$V_1 \cdot C_1 = V_2(D, G) \cdot C_2 \quad (5)$$

Setting  $D = D_f$  (thermal diffusivity of matrix),  $G$  approaches the critical thermal conductance,  $G_c$ .<sup>27</sup> The  $C_1$  values of STBNs were calculated by following the rule of mixtures with the heat capacity of both BN and silane compound, which were measured by differential scanning calorimeter (DSC). The resultant  $G_c$  values are summarized in Table II. The interfacial factor between BN3 and STBN3 was not calculated due to the higher oxygen content in BN3 fillers. This system was also excluded from the final estimation. The  $G_c$  values of STBN composite systems were higher than those of pristine BN systems, which means the thermal resistance at the interface was decreased by the surface modification. Consequently, we could show the effect of interfacial factor such as thermal resistance on the  $C_f$  parameter. In the meanwhile, we applied the same  $D_f$  value to both BN and STBN system due to the difficulty in calculation of  $D$  values. However, due to the improved the interfacial quality of STBN system, the real  $D$  values in STBN systems should be a little higher than those in BN systems. Therefore, our resultant  $G_c$  values of STBN system are slightly underestimated, giving lower ratio of  $G_c$  (STBN/BN) compared with  $C_f$  (STBN/BN).

### Estimating Thermal Conductivity

We have investigated the factors affecting the  $C_f$  parameters of eq. (1), which is related to the conductive pathways formation in the composite. From the results, the following relation can be suggested;

$$C_f \approx A(V) \cdot \text{Structure factor} \cdot \text{Interfacial factor} + B \quad (6)$$

The structure factor is about the microstructure of fillers in polymer matrix and represented by the inverse of the average contact number, which can be calculated by the simulation. The interfacial factor is about the thermal barrier at the filler–matrix interface and represented by the ratio of the thermal conductance.  $A(V)$  is the volume fraction-dependent value that can be calculated by the slope of  $C_f$  parameters according to their Structure factors at the specific volume fraction, as shown in Supporting Information Figure S7. The constant  $B$ , the intercept of linear lines in Supporting Information Figure S7, represents the infinite number of interface condition,

which is related to the thermal conductivity of matrix itself. For instance, at 13.5% volume fraction, BN2 system, which has the lowest  $C_f$  (0.826), shows the lowest representative value 0.337 that comes from the structure factor (0.337) multiplied by the interfacial factor (1.000), while STBN 1 system, which has the highest  $C_f$  (0.918), shows the highest value 0.431 that comes from the structure factor (0.424) multiplied by the interfacial factor (1.019). Those values of remaining cases are 0.424 and 0.344 for BN1 and STBN2, respectively. After considering constants  $A(V)$  and  $B$ , eq. (6) about the specific composite system can be obtained. Both structure and interfacial factors are denoted in Tables I and II. Consequently, we could estimate the  $C_f$  parameter of eq. (1) by calculating all those factors based on the characteristics of fillers, and the thermal conductivity of the composite could be anticipated by the eq. (1).

### CONCLUSIONS

In order to develop a new method to estimate the thermal conductivity of polymer composite, a model composite system composed of BN and HDPE was investigated by both experimental and simulation methods. Firstly, the effect of shape of fillers on a thermal conductivity was studied to find the best condition for fillers to form conductive networks. As a result, the composite system composed of fillers that have small average contact number has a tendency to show high thermal conductivity, and we could define those geometrical effects as “Structure factor”. Secondly, the effect of the interfacial thermal resistance between polymer and fillers was studied. The composite system having the reduced interfacial barrier showed the improved thermal conductivity, and we could define “Interfacial factor”. Eventually, we could quantify the  $C_f$  term of Agari and Uno equation, which is an index representing the degree of thermal conductance, by the characteristics of fillers denoted as “Structure factor” and “Interfacial factor”, ultimately permitting us to estimate the thermal conductivity of composite.

### ACKNOWLEDGMENTS

This work was financially supported by the Photo-electronic Hybrids Research Center of Korea Institute of Science and Technology (KIST). This research was also kindly supported by a grant from the Fundamental R&D Program for Technology of World Premier Materials funded by the Ministry of Knowledge Economy, Republic of Korea.

### REFERENCES

- Assael, M. J.; Antoniadis, K. D.; Metaxa, I. N. *J. Chem. Eng. Data* **2009**, *54*, 2365.
- Bogomolov, V. N.; Kartenko, N. F.; Kurdyukov, D. A.; Parfen'eva, L. S.; Smirnov, I. A.; Sharenkova, N. V.; Misiorek, H.; Jezowski, A. *Phys. Solid. State* **2003**, *45*, 957.
- Han, S.; Lin, J. T.; Yamada, Y.; Chung, D. D. L. *Carbon* **2008**, *46*, 1060.
- Zhang, Y.; Ong, N. P.; Anderson, P. W.; Boon, D. A.; Liang, R.; Hardy, W. N. *Phys. Rev. Lett.* **2001**, *86*, 890.
- Zhi, C. Y.; Xu, Y. B.; Bando, Y.; Golberg, D. *ACS Nano* **2011**, *5*, 6571.
- Bujard, P.; Kuhnlein, G.; Ino, S.; Shiobara, T. *IEEE T Compon. Pack A* **1994**, *17*, 527.

7. Lee, G. W.; Park, M.; Kim, J.; Lee, J. I.; Yoon, H. G. *Compos. Part A-Appl. Sci.* **2006**, *37*, 727.
8. Ruh, R.; Donaldson, K. Y.; Hasselman, D. P. H. *J. Am. Ceram. Soc.* **1992**, *75*, 2887.
9. Tavman, I. H. *Int. Commun. Heat Mass* **1998**, *25*, 723.
10. Terao, T.; Zhi, C. Y.; Bando, Y.; Mitome, M.; Tang, C. C.; Golberg, D. *J. Phys. Chem. C* **2010**, *114*, 4340.
11. Ye, C. M.; Shentu, B. Q.; Weng, Z. X. *J. Appl. Polym. Sci.* **2006**, *101*, 3806.
12. Yu, A. P.; Ramesh, P.; Itkis, M. E.; Bekyarova, E.; Haddon, R. C. *J. Phys. Chem. C* **2007**, *111*, 7565.
13. Ishida, H.; Rimdusit, S. *Thermochim. Acta* **1998**, *320*, 177.
14. Li, Y.; Huang, X. Y.; Hu, Z. W.; Jiang, P. K.; Li, S. T.; Tanaka, T. *ACS Appl. Mater. Inter.* **2011**, *3*, 4396.
15. Wattanakul, K.; Manuspiya, H.; Yanumet, N. *J. Compos. Mater.* **2011**, *45*, 1967.
16. Song, F.; Zhao, H. F.; Hu, G. K. *Comp. Mater. Sci.* **2012**, *51*, 353.
17. Hu, L.; Desai, T.; Koblinski, P. J. *Appl. Phys.* **2011**, 110.
18. Clancy, T. C.; Frankland, S. J. V.; Hinkley, J. A.; Gates, T. S. *Int. J. Therm. Sci.* **2010**, *49*, 1555.
19. Zhou, Y. C.; Wang, H.; Xiang, F.; Zhang, H.; Yu, K.; Chen, L. *Appl. Phys. Lett.* **2011**, 98.
20. Wang, M.; Kang, Q. J.; Pan, N. *Appl. Therm. Eng.* **2009**, *29*, 418.
21. Agari, Y.; Uno, T. *J. Appl. Polym. Sci.* **1986**, *32*, 5705.
22. Agari, Y.; Ueda, A.; Nagai, S. *J. Appl. Polym. Sci.* **1993**, *49*, 1625.
23. Richard, R. G.; Shankland, I. R. *Int. J. Thermophys.* **1989**, *10*, 673.
24. Vozar, L. J. *Therm. Anal.* **1996**, *46*, 495.
25. Samuels, R. J.; Mathis, N. E. *J. Electron. Packaging* **2001**, *123*, 273.
26. Lee, G. W.; Lee, J. I.; Lee, S. S.; Park, M.; Kim, J. *J. Mater. Sci.* **2005**, *40*, 1259.
27. Wilson, O. M.; Hu, X. Y.; Cahill, D. G.; Braun, P. V., *Phys. Rev. B* **2002**, 66.
28. Samuels, R. J.; Mathis, N. E. *J. Electron. Packaging* **2001**, *123*, 273.
29. Yuan, G. M.; Li, X. K.; Dong, Z. J.; Westwood, A.; Cui, Z. W.; Cong, Y.; Du, H. D.; Kang, F. Y. *Carbon* **2012**, *50*, 175.
30. Marconnett, A. M.; Yamamoto, N.; Panzer, M. A.; Wardle, B. L.; Goodson, K. E., *ACS Nano*. **2011**, *5*, 4818.
31. Pettersson, S.; Mahan, G. D. *Phys. Rev. B* **1990**, *42*, 7386.
32. Shenogin, S.; Bodapati, A.; Xue, L.; Ozisik, R.; Koblinski, P. *Appl. Phys. Lett.* **2004**, *85*, 2229.